for large matrices. It has been demonstrated that the use of boundary conditions appropriate at a large distance from the duct exit may cause reflections and steady-state error when applied on an artificial truncated boundary at a moderate distance from the exit. Work is presently continuing on an iterative procedure for the far-field boundary condition. Primarily, it consists of treating the pressure at each point on the far-field boundary as locally one-dimensional. The boundary condition is applied so as to pass the one-dimensional pressure wave without reflection. A related approach has been used by Baumeister and Horowitz.[6] In their work, the acoustic impedance along the far-field boundary is iteratively adjusted to minimize reflection.

References

[1]Baumeister, K.J., "Numerical Techniques in Linear Duct Acoustics—A Status Report," *Journal of Engineering for Industry,* Vol. 103, No. 3, 1981, pp. 270-281.

[2]Thompson, J.F., "Numerical Solution of Flow Problems Using Body-Fitted Coordinate Systems," *Computational Fluid Dynamics,* Vol. 1, edited by W. Kollman, Hemisphere Publishing Corp., New York, 1980, pp. 1-98.

[3]White, J.W., "A General Mapping Procedure for Variable Area Duct Acoustics," *AIAA Journal,* Vol. 20, July 1982, pp. 880-884.

[4]Bayliss, A. and Turkel, E., "Radiation Boundary Conditions for Wave-Like Equations," *Communications on Pure and Applied Mathematics,* Vol. 33, 1980, pp. 707-725.

[5]Warming, R.F. and Beam, R.M., "On the Construction and Application of Implicit Factored Schemes for Conservation Laws," *SIAM-AMS Proceedings,* Vol. II, 1978, pp. 85-129.

[6]Baumeister, K.J. and Horowitz, S.J., "Finite Element-Integral Simulation of Static and Flight Fan Noise Radiation from the JT15D Turbofan Engine," NASA TM 82936, Nov. 1982.

Flow from Sharp-Edged Rectangular Orifices—The Effect of Corner Rounding

A. Pollard and M. A. Iwaniw†
Queen's University, Ontario, Canada

Introduction

THE free jet flows from sharp-edged rectangular orifices exhibit saddle-backed velocity distributions in the plane of the orifice major axis.[1-10] The maximum magnitude of these velocity excesses is typically 20% greater than the local mean centerline velocity (U_{ℓ}). Moreover, they occur in the region between the merging of the shear layers from the long sides of the orifice and the merging of the shear layers from the short sides of the orifice (i.e., $3 \leq x/t_p \leq 30$, for slot aspect ratio $\ell/t_p = 10$).

Although there has been, and continues to be, much discussion in the literature about the cause(s) for the occurrence of the saddle-backed velocity profile,[1-16] it is the author's opinion that no clear consensus has emerged. A reader interested in a comprehensive review of the literature is referred to Ref. 17.

In studies to date, the rectangular orifice plates have possessed sharp, 90-deg corner regions. These corner regions are, of course, the start of the interaction between the two sets of shear layers that originate along the short and long sides of the orifice. Although various gometrical alterations have been made to the orifices, such as upstream shaping[6] or the attachment of channels downstream of the orifice,[6,9] the effect of corner rounding on the appearance, magnitude, and location of these saddle-backed velocity distributions has not been addressed.

The purpose of this Note is to determine the effect of rounding the corners of a rectangular sharp-edged orifice on the location and magnitude of the saddle-backed velocity profiles. This is accomplished by reference to some previously published work[10,16] that used the same orifice but with sharp 90-deg corners (see Fig. 1).

Experiments

Laboratory air was supplied to a settling chamber by a fan. The rectangular orifice was attached to the downstream face of the settling chamber. This downstream face was flush with a large plywood wall to ensure that entrainment at the nozzle exit plane was normal to the jet centerline. The top and sides of the rig were covered with 1.59-mm mesh wire screen to prevent large-scale movement of air (room drafts) into the jet.

The experiments were performed in a $9.02 \times 7.39 \times 3.76$ m room into which traffic was strictly controlled. Check of ambient flow conditions verified the hypothesis that external disturbances and those produced by the jet itself were indeed very small.

The bilateral symmetry of the flow was utilized in acquiring data and checks were made to ascertain that symmetry did, in fact, exist in the two planes containing the major and minor axes of the orifice.

The orifices used are shown schematically in Fig. 1. These orifices were manufactured in accordance with British Standards for orifice plates (BS 1042). The sharp-corner orifice was made from four intersecting plates. The rectangular, sharp-edged, round-corner orifice is shown superimposed in the figure. Note that the area of the round-corner orifice is

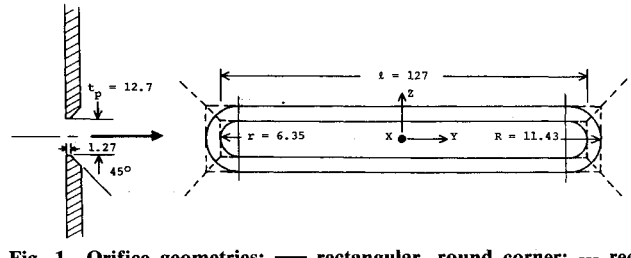

Fig. 1 Orifice geometries: — rectangular, round corner; --- rectangular, sharp corner.[10,16,17] (all dimensions in mm).

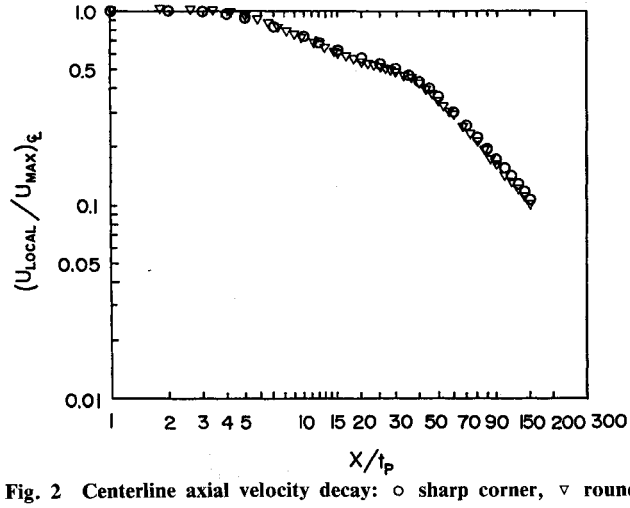

Fig. 2 Centerline axial velocity decay: ○ sharp corner, ▽ round corner.

Received Dec. 8, 1983; revision submitted April 23, 1984.

*Associate Professor, Department of Mechanical Engineering.
†Research Assistant, Department of Mechanical Engineering.

about 98% of the sharp-corner orifice, both with an aspect ratio of 10.

The Reynolds number of the flow from the sharp-corner orifice, based on the orifice height (t_p) and mean axial velocity at the jet centerline ($U_0 = 55$ m/s), was about 47,000. For the round-corner orifice, the Reynolds number, based on the same variables, was about 40,000. This change in Re is not expected to alter the flow situation to any detectable degree; see, for example, Ref. 2.

Further details of the experimental methodology, calibration, equipment, etc., can be found in Refs. 10, 16, and 17.

Presentation and Discussion of Results

Data for the mean axial velocity centerline decay are shown in Fig. 2. This figure shows the results from using the round-corner orifice and the previously published results from a sharp-corner orifice. Four distinct regions can be identified: the potential core region $1 \le x/t_p \le 3$; the characteristic decay region $3 \le x/t_p \le 30$; the transition region $30 \le x/t_p \le 60$; and the final decay region $x/t_p \ge 60$. The slopes of the velocity decay in the final decay region are -1.11 for the sharp-corner orifice[16] and -1.15 for the round-corner orifice. It may be of interest to note than when replotted in the form $U_0/U_\ell = A(x/D_e - B)$, where B is the kinematic virtual origin for data at $x/D_e \ge 17$ ($x/t_p \ge 60$) and D_e is the equivalent diameter for an axisymmetric orifice of the same area, it is found that $A = 0.256$ and $B = 3.42$ for the round-corner orifice ($A = 0.253$ and $B = 5.06$ for the sharp-corner orifice[17]). The slope of this curve is much larger than the 0.16 obtained for the self-preserving round jet flow,[18] implying a much greater rate of entrainment than for a round jet.

The mean axial velocity profiles in the x-y plane are shown in Fig. 3. Although not shown, data for (essentially) the same stations downstream of the sharp-corner orifice compare well with these. The saddle-backed velocity profiles are clearly observed; moreover, the locations and the magnitudes of these velocity excesses are found to be in accord for both sharp- and round-corner orifices (i.e., within 2%). It is also clear that the velocity excesses lie within the characteristic decay region (i.e., $3 \le x/t_p \le 30$).

The mean axial velocities in the transverse centerplane direction (i.e., z direction) were also taken, but are not given here for reasons of brevity. The profiles, however, were found to be within the aforementioned error bound, the same as those obtained using a sharp-corner orifice.

Attention is now turned to axial turbulence intensities. The centerline intensities in the x, y, z directions for the sharp-corner orifice[16] and those in the x direction for the round-corner orifice are plotted in Fig. 4. It can be said that there is little difference in the axial (u) turbulence-intensity results. The variation of $(\overline{u'^2})^{1/2}$ with downstream distance can be linked with the orifice exit conditions. The reader is referred to Refs. 9, 19, and 20 for details regarding the general behavior of these profiles. Figure 5 provides the profiles of the axial turbulence intensities in the lateral (y-x) direction for the round-corner orifice. These data, when compared to those from the sharp-corner orifice,[16] indicate that the longitudinal turbulence-intensity distribution is essentially the same for both orifices. At $x/t_p = 10$ there is a depression in the intensities (this behavior is also vividly observed at $x/t_p = 5$, however, not shown here). This depression is not seen at downstream distances greater than 10. In Ref. 16, it was noted that these depressions were located in a region where zero values of $u'v'$ and the zero gradient of the mean axial velocities were not coincident; nor were the mean velocity profiles symmetric about the saddle-back peaks. These new data display similar behavior, and thus open the possibility that, in this jet, as in the former case,[16] there may exist regions of turbulence suppression or negative production.[21]

The transverse direction (z-x plane) turbulence intensities have also been taken, but are also not shown for reasons of brevity. As in the sharp-corner orifice case, the axial development of these profiles shows no evidence of negative production; and, within the characteristic decay region ($3 \le x/t_p \le 30$), those profiles appear self-similar.

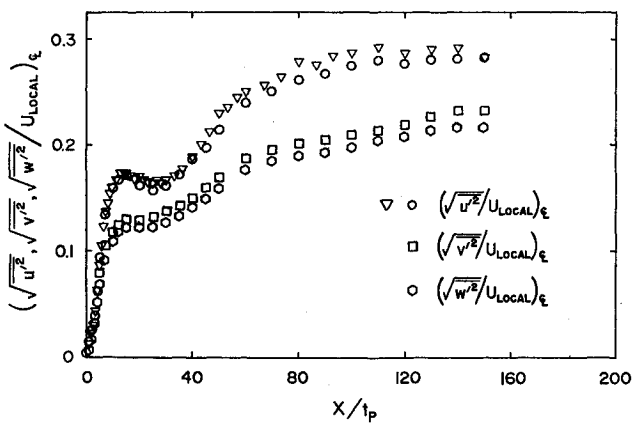

Fig. 4 Centerline turbulence intensity: ○, □, ◇ sharp-corner orifice[16]; ▽ round-corner orifice.

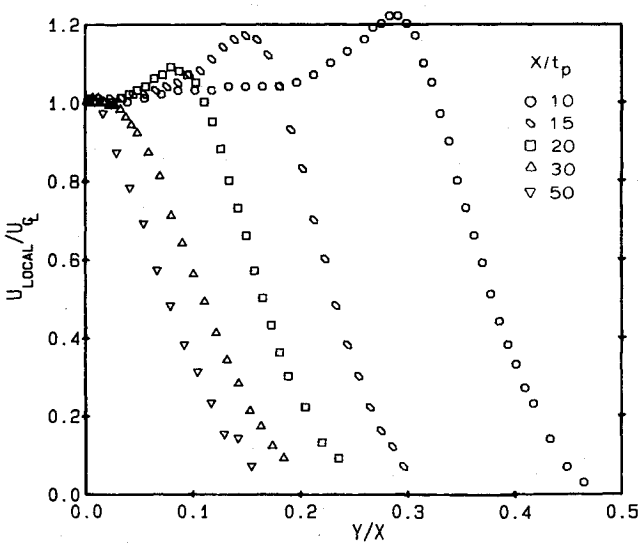

Fig. 3 Axial velocity profiles in lateral direction (round corner orifice).

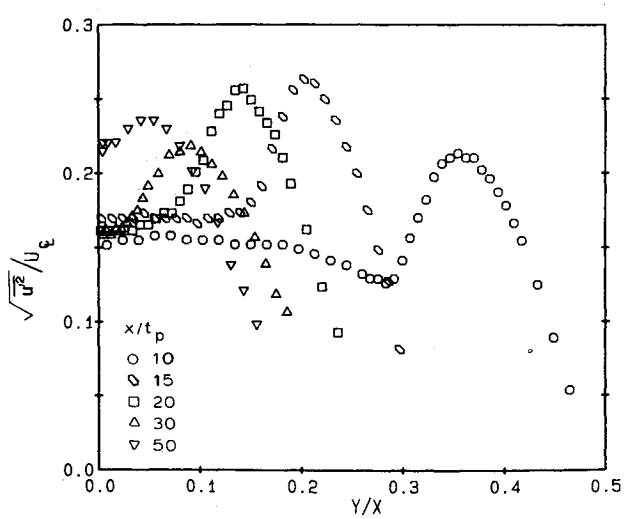

Fig. 5 Axial turbulence intensity profiles in lateral direction (round-corner orifice).

Conclusions

New data have been obtained for the flow issuing from a round-corner sharp-edged rectangular orifice. When compared to the previously published data from a similar orifice, but with sharp corners, these new data show that the round corners have no discernible effect upon either the magnitude or location of the saddle-back velocity profile.

Acknowledgments

This work has been supported by a grant from the Natural Science and Engineering Research Council of Canada. A more complete version of this paper can be obtained from the leading author.

References

[1]Van der Hegge Zijnen, B. G., "Measurements of the Velocity Distribution in a Plane Turbulent Jet of Air," *Applied Scientific Research*, Sec. A, Vol. 7, 1958, pp. 256-276.

[2]Sforza, P. M., Steiger, M. H., and Trentacoste, N., "Studies on Three-Dimensional Free Jets," *AIAA Journal*, Vol. 4, May 1966, pp. 800-806.

[3]Trentacoste, N. and Sforza, P. M., "Further Experimental Results for Three-Dimensional Free Jets," *AIAA Journal*, Vol. 5, May 1967, pp. 885-891.

[4]Sfeir, A. A., "The Velocity and Temperature Fields of Rectangular Jets," *International Journal of Heat and Mass Transfer*, Vol. 19, 1976, pp. 1289-1297.

[5]Sfeir, A. A., "Investigation of Three-Dimensional Turbulent Rectangular Jets," *AIAA Journal*, Vol. 17, Oct. 1979, pp. 1055-1060.

[6]Marsters, G. F., "The Effects of Upstream Nozzle Shaping on Incompressible Turbulent Flows from Rectangular Nozzles," *Transactions of CSME*, Vol. 4, 1978/79, pp. 197-203.

[7]Marsters, G. F., "An Experimental Investigation of Spanwise Velocity Distribution in Jets from Rectangular Orifices," AIAA Paper 80-0202, 1980.

[8]Marsters, G. F., "Spanwise Velocity Distributions in Jets from Rectangular Slots," *AIAA Journal*, Vol. 19, Feb. 1981, pp. 148-152.

[9]Krothapalli, A., Baganoff, D., and Karamcheti, K., "On the Mixing of a Rectangular Jet," *Journal of Fluid Mechanics*, Vol. 107, 1981, pp. 201-220.

[10]Quinn, W. R., Pollard, A., and Marsters, G. F., "On Saddle-Backed Velocity Distributions in a Three-Dimensional Turbulent Free Jet," AIAA Paper 83-1677, July 1983; also, submitted for publication in *AIAA Journal*.

[11]Viets, H. and Sforza, P. M., "Dynamics of Bilaterally Symmetric Vortex Rings," *Physics of Fluids*, Vol. 15, No. 2, 1972, pp. 230-240.

[12]Birch, S. F., "The Effect of Initial Conditions on High Reynolds Number Jets," AIAA Paper 83-1681, 1983.

[13]Sforza, P. M. and Smoto, M., "Predictions of Three-Dimensional Heated Turbulent Jet Flow Fields," *Proceedings, Numerical Methods in Thermal Problems*, Pineridge Press, Swansea, U.K., 1979, pp. 903-912.

[14]McGuirk, J. J., and Rodi, W., "The Calculation of Three-Dimensional Turbulent Free Jets," *Ist Symposium on Turbulent Shear Flows*, University Park, Pa., Vol. 1, April 1977, pp. 1.29-1.36.

[15]Abramovich, G. N., "On the Deformation of the Rectangular Turbulent Jet Cross-Section," *International Journal on Heat and Mass Transfer*, Vol. 25, 1982, pp. 1885-1894.

[16]Quinn, W. R., Pollard, A., and Marsters, G. F., "Measurements in a Turbulent Rectangular Free Jet," *Proceedings, Fourth Symposium Turbulent Shear Flows*, Karlsruhe, 1983, pp. 7.1-7.6.

[17]Quinn, W. R., "Turbulent Jet Flow from a Sharp-Edged Rectangular Slot," Ph.D. Thesis, Department of Mechanical Engineering, Queen's University, Ontario, Canada, 1984.

[18]Rodi, W., "A New Method of Analyzing Hot Wire Signal in Highly Turbulent Flow, and its Evaluation in a Round Jet," *DISA Information*, Vol. 17, 1975, pp. 9-18.

[19]Hussain, A.K.M.F. and Clark, A. R., "Upstream Influence of the Near Field of a Plane Turbulent Jet," *Physics of Fluids*, Vol. 20, 1977, pp. 1416-1426.

[20]Hill, W. G., Jenkins, R. C., and Gilbert, B. L., "Effects of the Initial Boundary Layer State on Turbulent Jet Mixing," *AIAA Journal*, Vol. 14, 1976, pp. 1513-1514.

[21]Hinze, J. O., "Turbulent Flow Regions with Shear Stress and Mean Velocity Gradient of Opposite Sign," *Applied Scientific Research*, Vol. 22, 1970, p. 163.

Harmonic Temperature Effect on Vibrations of an Orthotropic Plate of Varying Thickness

J. S. Tomar* and A. K. Gupta†
University of Roorkee, Rookee, India

Introduction

THE interest in the effect of temperature on solid bodies has increased as a result of recent developments in space technology, high-speed atmospheric flights, and nuclear energy applications. Notable contributons are available on the vibrations of orthotropic rectangular plates.[1-4] It is well known[5] that, in the presence of a constant thermal gradient, the elastic coefficients of homogeneous materials become functions of the space variable. Fanconneau and Marangoni[6] have investigated the effect of the nonhomogeneity caused by a thermal gradient on the natural frequencies of a simply supported plate of uniform thickness. Recently, Tomar and Gupta[7,8] have considered the effect of a thermal gradient on the frequencies of an orthotropic plate of variable thickness. The object of this study is to determine the effect of the harmonic temperature distribution on the frequencies of an orthotropic rectangular plate of linearly varying thickness. Here, the quintic spline technique has been used to compute the frequencies for the first two modes of vibration for different combinations of boundary conditions and for various values of aspect ratio, taper constant, and temperature constant.

Analysis and Equation of Motion

It is assumed that the rectangular orthotropic material is subjected to an harmonic temperature distribution along its length, i.e., in the x direction

$$T = T_0 \cos(\pi/2)x \tag{1}$$

where T denotes the temperature excess above the reference temperature at any point at a distance $X = x/a$ and T_0 the temperature excess above the reference temperature at the end $x = a$ or $X = 1$.

The temperature dependence of the modulus of elasticity for most orthotropic materials is given by

$$E_x(T) = E_1(1-\gamma T),\ E_y(T) = E_2(1-\gamma T),\ G_{xy}(T) = G_0(1-\gamma T) \tag{2}$$

where E_1 and E_2 are the values of Young's moduli in the x and y directions, respectively, and G_0 the value of the shear modulus between directions x and y at the reference temperature, i.e., at $T = 0$.

Taking as a reference the temperature at the end of the plate, i.e., at $X = 1$, the modulus variations in view of Eqs. (1) and (2) become

$$E_x(X) = E_1[1-\alpha\cos(\pi/2)X],\ E_y(X) = E_2[1-\alpha\cos(\pi/2)X]$$

$$G_{xy}(X) = G_0[1-\alpha\cos(\pi/2)X] \tag{3}$$

where $\alpha = \gamma T_0 (0 \le \alpha < 1)$, a parameter representing the temperature constants.

Received Nov. 14, 1983; revision received April 12, 1984.

*Professor, Department of Mathematics.
†Research Fellow, Department of Mathematics.